Thermal analysis of a multi-layer microchannel heat sink for cooling concentrator photovoltaic (CPV) cells

Idris Al Siyabi, Katie Shanks, Tapas Mallick, and Senthilarasu Sundaram

Citation: AIP Conference Proceedings **1881**, 070001 (2017); doi: 10.1063/1.5001434

View online: https://doi.org/10.1063/1.5001434

View Table of Contents: http://aip.scitation.org/toc/apc/1881/1

Published by the American Institute of Physics

Thermal Analysis of a Multi-Layer Microchannel Heat Sink for Cooling Concentrator Photovoltaic (CPV) Cells

Idris Al Siyabi[a)], Katie Shanks, Tapas Mallick and Senthilarasu Sundaram

Environment and Sustainability Institute, University of Exeter, Penryn, UK TR10 9EZ

[a)]Corresponding author: ia257@exeter.ac.uk

Abstract. Concentrator Photovoltaic (CPV) technology is increasingly being considered as an alternative option for solar electricity generation. However, increasing the light concentration ratio could decrease the system output power due to the increase in the temperature of the cells. The performance of a multi-layer microchannel heat sink configuration was evaluated using numerical analysis. In this analysis, three dimensional incompressible laminar steady flow model was solved numerically. An electrical and thermal solar cell model was coupled for solar cell temperature and efficiency calculations. Thermal resistance, solar cell temperature and pumping power were used for the system efficiency evaluation. An increase in the number of microchannel layers exhibited the best overall performance in terms of the thermal resistance, solar cell temperature uniformity and pressure drop. The channel height and width has no effect on the solar cell maximum temperature. However, increasing channel height leads to a reduction in the pressure drop and hence less fluid pumping power.

INTRODUCTION

Concentrating photovoltaic (CPV) technology has gained much attention especially with high concentration, because of its competitive cost [1]. Studies show that the solar cell temperature could reach 1400°C under 500 concentration ratio if it is fully insulated [2]. The increase of solar cell temperature more than the manufacturer specified temperature will result in a decrease of its efficiency in the order of 0.45% per °C and can cause long-term degradation if it exceeds the maximum limit [3]. Also, non-uniform solar cell temperature can decrease its electrical efficiency [4]. Therefore, solar cell temperature regulation should be considered in any CPV system design by removing the generated heat efficiently. Solar cell arrangements are classified as single-cell, linear and densely packed cells [5]. It has been found that CPV single solar cells can be cooled using passive techniques of less than 1.7K/W heat sink thermal resistance but in extreme outdoor conditions lower thermal resistance is needed (1.4 K/W) [6]. However, a passive heat sink with lower thermal resistance would be large in size requiring more space. For a single solar cell array, the large heat sink will increase the overall system weight and space which necessitates a stronger structure and also larger motor for the tracking system. Therefore, an active cooling system might be a viable solution for a single solar cell receiver array in terms of overall system efficiency.

Various active cooling techniques have been studied for a single solar cell in a CPV systems. Aldossary et al. [7] has examined the active cooling on 1cm² solar cell under high concentration ratio(500×) using a rectangular cooling channel with 10mm height. The solar cell maximum surface temperature was maintained at 60°C for 0.01 m/s water velocity with heat transfer coefficient of 1645 W/(m²K). Reddy et al. [8] has carried out a numerical analysis of a microchannel heat sink for a 1.5 kw_e HCPV receiver. It was found that only 0.2% of the produced power by the CPV module is needed for pumping water. Barrau et al. [9] has designed a hybrid jet impingement/microchannel cooling system for a densely packed CPV module. Low thermal resistance (up to 6.2×10^{-5} K/W) and a uniform temperature across the receiver was achieved.

A stacked micro channel heat sink technique is considered more efficient in terms of pumping power and heat removal capability [10]. However, the thermal performance of a stacked microchannel heat sink depends on the geometry(channel depth, width and length), materials and operation conditions(flow rate) [11]. Therefore, applying

13th International Conference on Concentrator Photovoltaic Systems (CPV-13)
AIP Conf. Proc. 1881, 070001-1–070001-8; doi: 10.1063/1.5001434
Published by AIP Publishing. 978-0-7354-1561-4/$30.00

a multi-layer microchannel heat sink in a CPV cooling application requires special attention due to the rapid temperature increase in CPV technology.

In this paper, a numerical analysis of a multi-layer microchannel heat sink cooling system for a high concentration single solar CPV receiver has been carried out. The analysis includes various multi-layer heat sink configurations to determine the most efficient option in terms of cell temperature and fluid pumping power. The geometry of the channel has also been explored.

SYSTEM MODEL DESCRIPTION

The modeled system, illustrated in figure 1, consists of a CPV multi-junction (MJ) solar cell assembly (AZURSPACE 3C42) and a multi-layer microchannel heat sink. The CPV MJ solar cell assembly consists of a solar cell located under a conductive layer made of copper. A ceramic layer placed under the copper layer is used as electrical insulation. Finally, the full arrangement is placed in a second copper layer for thermal conduction purposes. The assembly also consists of two by-pass diodes and two electrical terminals. However for simplicity, the diodes are not considered in the model. All the CPV assembly dimensions, thickness and materials are listed in table 1 [7]. The solar cell size is 10mm×10mm and is made of GalnP-GalnAs-Ge. The electrical efficiency of the solar cell under concentration ratio of 500× and standard test conditions (CSTC) is 41.2%.

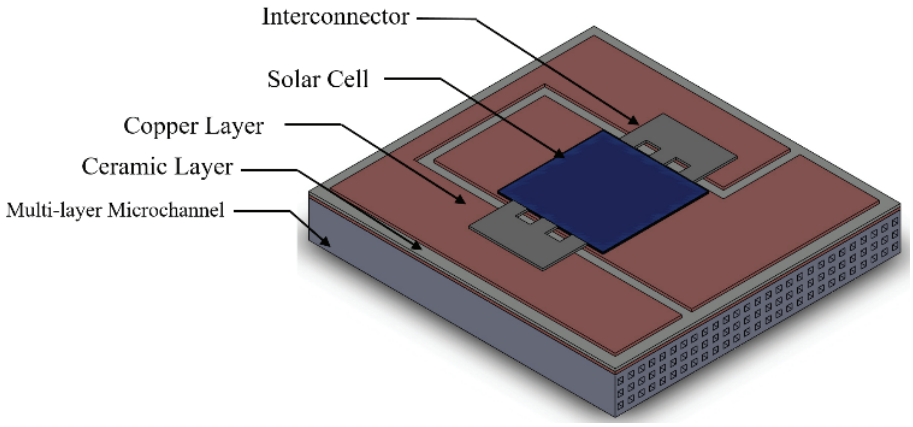

FIGURE 1. The multi-layer microchannel heat sink and CPV receiver schematic diagram.

TABLE 1. The CPV receiver dimensions and its material thermophysical properties.

Layer	Dimension (mm)	Thickness (mm)	Thermal conductivity (W/mK)	Heat Capacity (J/kgK)	Density (kg/m³)
GalnP	10×10	0.066	73	370	4470
GalnAs	10×10	0.067	65	550	5316
Ge	10×10	0.067	60	320	5323
Copper I	27×25	0.250	400	385	8700
Ceramic	29×27	0.320	27	900	3900
Copper II	29×27	0.250	400	385	8700
Aluminum	-	-	160	900	2700
Solder	-	0.125	50	150	9000
Silver	-	0.20	430	235	10490

A typical multi-layer microchannel heat sink design is shown in figure 2. All layers are stacked in an arrangement with parallel fluid flow. The overall heat sink dimension are 29mm ×27mm (L×W). Different heat sinks have been considered in terms of channel width (W_c), channel height (H_c) and fins width (W_f) as shown in table 2 and figure 2. The top plate thickness (t_{b1}), bottom base thickens (t_{b2}) and plate thickness between layers (t_b) are kept the same for all heat sinks to 500 μm.

TABLE 2. The multi-layer heat sink dimensions in the present study.

Heat sink#	Width of fin W_f (µm)	Width of channel W_c(µm)	Depth of channel H_c(µm)
1	500	500	500
2	700	700	500
3	1000	1000	500
4	500	500	750
5	500	500	1000

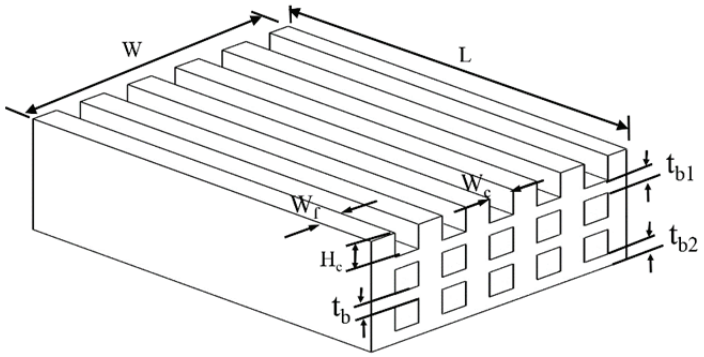

FIGURE 2. Dimensions of the multi-layer microchannel representation: spacing (W_c), fins height (H_c), thickness (W_f), length (L), base width (W), base thickness (tb, tb_1, tb_2)

The thermal boundary conditions of the studied model are shown in figure 3 and table 3. Also, the following assumptions have been considered:

- The solar cell is subjected to a uniform solar radiation of 1000W/m² and concentration ratio of 500 suns and all heat is produced by the Ge subcell [6].
- The ambient temperature is 25°C.
- Water is selected as the coolant fluid and its properties varies with temperature [12,13].Water inlet temperature is 25°C.
- Water total mass flow rate is 0.002 kg/s which corresponds to low Reynolds numbers. The flow is steady, laminar and fully developed in each channel.

TABLE 3. The model thermal boundary conditions.

No	Region	Boundary Condition
1	CPV top surfaces	Natural convection(15W/m²K)
2	Germanium Subcell	Heat source (Q_h)
3	Surfaces on bottom and sides of heat sink	Thermally insulated

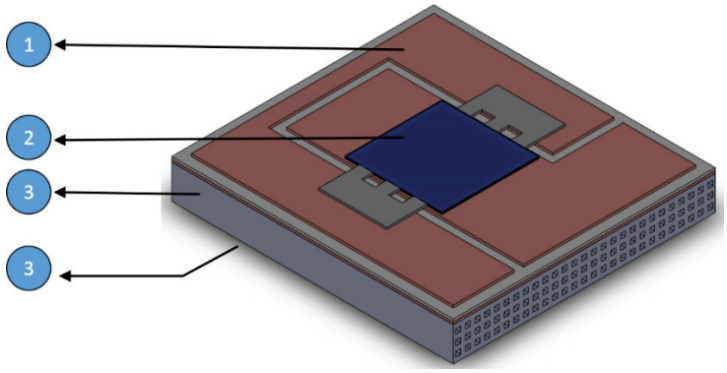

FIGURE 3. Schematic of the computational domain and boundary conditions.

NUMERICAL ANALYSIS

COMSOL Multiphysics (version 5.2) was used to build a 3D numerical model using non-isothermal flow physics [14]. The simulations are conducted in steady state study conditions. Concentrated solar irradiation falls uniformly over the outer solar cell subcell. Each solar cell subcell generates electricity based on the wavelength. The lower solar cell subcell (germanium) is considered as the heat source [6]. The total heat generated by the system per m² (Q_h) can be expressed as:

$$Q_h = (1-\eta_{elec})Q_o \tag{1}$$

Where Q_o indicates the total optical power in W at the outlet of the concentrator and η_{elec} is the electrical efficiency of the solar cell. The optical power takes into account both the concentration ratio and the concentrator efficiency. The solar cell manufacturer has specified the typical solar cell electrical efficiency at 500× versus temperature [15]. The electrical efficiency can be expressed using a linear relation with temperature as the following:

$$\eta_{elec}(T) = -5.09\times10^{-4}T + 0.40227 \tag{2}$$

Where T is the solar cell temperature between 25°C and 80°C, all CPV assembly top surfaces release heat to the environment using natural convection mode and the convection heat transfer rate (q_{conv}) is given by:

$$q_{conv} = h.A.\Delta T \tag{3}$$

Where h is the convection heat transfer coefficient (W/m²K), A is the exposed surface area (m²) and ΔT is the temperature difference between the top surface and the ambient (K). Also, the heat is transferred to the environment by radiation and its transfer rate (W) is expressed by:

$$q_{rad} = \varepsilon.\sigma.A.(T_{rad}^4 - T_{amb}^4) \tag{4}$$

Where ε is the emissivity of the materials, σ is Stefan-Boltzmann constant, A is the radiated surface area, T_{surf} is the surface area and T_{amb} is the ambient temperature. However, most of the generated heat is transferred to the lower part of the CPV assembly and then to the heat sink by conduction phenomena.

In multi-layer microchannel heat sink, each single microchannel is assigned with an individual fluid inlet and outlet. The coolant fluid is pumped through the channels at mass flow rate (kg/s) and atmospheric pressure is assigned to the outlet. The conservation of mass, momentum and energy governing equations can be described as in [13].

The heat sink performance can be investigated using two parameters: total thermal resistance and fluid pumping power. The total thermal resistance (R_{th}) can be expressed as:

$$R_{th} = \frac{\Delta T_{\max}}{qA_s} \tag{5}$$

Where q is the heat flux, A_s is the heat sink surface area and ΔT_{max} is the temperature difference between the fluid inlet and the heat sink maximum temperature and defined as:

$$\Delta T_{\max} = T_{s,\max} - T_{f,in} \tag{6}$$

Where $T_{s,max}$ is the maximum temperature of the heat sink i.e. the solar cell maximum temperature and $T_{f,in}$ is the fluid inlet temperature. The fluid pumping power is another measure of the heat sink efficiency and can be calculated for each microchannel using the equation below:

$$P_{ch} = u_{avg}.A_c.\Delta p \tag{7}$$

Where u_{avg} is the fluid average velocity, A_c is the sectional area of the channel and Δp is the pressure drop along the microchannel.

RESULTS AND DISCUSSION

The computational domain was meshed using a free tetrahedral grid system. In order to confirm that the solution is independent of the size of the mesh for each case, it was performed with different mesh sizes. As an example, figure 4 shows the average and maximum solar cell temperature changes with the number of elements for two layer micro channel heat sink. The number of elements has been varied between 0.25×10^6 and 2.5×10^6. The maximum

and average solar cell temperatures are constant for the number of elements between 1.76×10^6 and 2.5×10^6. Therefore, the number of elements with 1.76×10^6 has been selected for 2 layer microchannel heat sink.

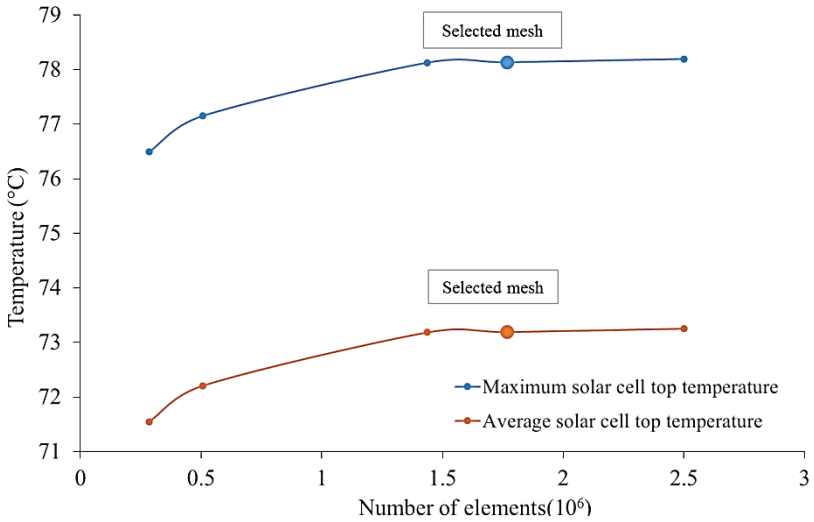

FIGURE 4. Grid Independence study for 2 number of layers microchannel heat sink with channel cross section 500×500μm.

As mentioned earlier, the solar cell efficiency decreases with temperature increase. Therefore, a trial and error iteration approach has been used to find the solar cell temperature at the steady state condition, the solar cell temperature being initially assumed equal to the ambient temperature. Equations (2) and (1) are used to find the solar cell efficiency and the generated heat by the solar cell respectively. The model is then solved based on this assumption and a new solar cell temperature is found. The new temperature is used to calculate the electrical efficiency and hence the generated heat and the model is solved again. The process is repeated until the solar cell temperature difference reaches the allowable limit of ≤0.01°C. Figure 5 shows the variations in the average solar cell temperature with iterations for the various number of layer heat sinks for the channel size of 500×500μm. The temperature difference becomes below the limit after the 4^{th} iteration in all cases.

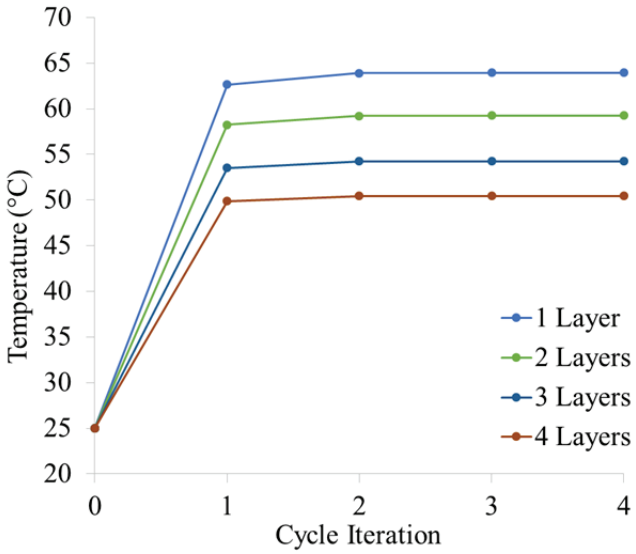

FIGURE 5. Variation of solar cell average temperature with cycle iteration for 500×500μm channel cross section and 0.002 kg/s water flow rate.

Any water cooled heat sink performance is usually evaluated by two parameters, thermal resistance and pumping power. The effect of the numbers of layers in the heat sink has been investigated for the same channel cross section (500×500μm) and 0.002kg/s water mass flow rate. As shown in Figure 6 (a), the heat sink thermal resistance and the solar cell maximum temperature both decrease with the increase of the numbers of layers for the same water mass flow rate. The maximum solar cell temperature was maintained below 69°C for all the heat sink arrangements.

The increase of the number of layers in the heat sink leads to a lowering in the fluid mass flow rate in each channel and reduces the pressure drop along the channel. Figure 6 (b) shows that the heat sink total pressure drop has been reduced by 50% when using the two layer heat sink compared to the single layer heat sink pressure drop. However, the pressure drop starts to decrease slightly for the three and four layer heat sinks. In addition, the pumping power has been reduced significantly for the double layer heat sink compared to the single heat sink layer but the change in the pumping power is slightly decreased for the three and four layers compared to double number of layer heat sink.

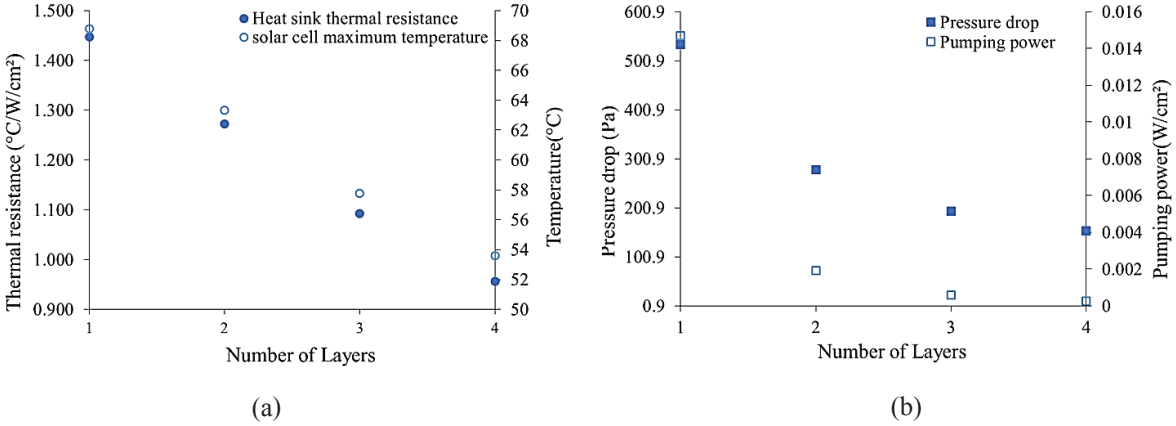

FIGURE 6. Effects of the number of microchannel layers for 500×500μm channel cross section (a) the thermal resistance and the maximum solar cell temperature (b) the total heat sink pressure drop and the required fluid pumping power.

The temperature on the solar cell surface has to be uniform for maximum electrical efficiency. Figure 7 shows the temperature distribution in the solar cell surface for different number of layer heat sinks. It can be observed that the maximum temperature zone in the solar cell surface is located at the outlet fluid side. Also, the increase of the number of layers reduces the temperature non-uniformity of the solar cell by 6°C between the one and three layer arrangement.

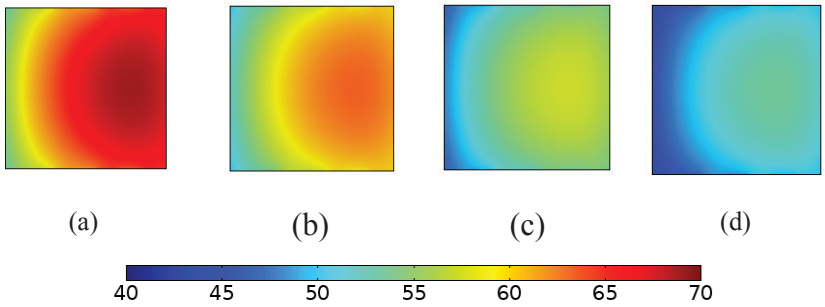

FIGURE 7. Solar cell surface temperature for 500×500μm channel cross section and 0.002 kg/s flow rate for (a) one layer, (b) two layer, (c) three layer and , (d) four layer heat sink.

The aspect ratio value is defined as the ratio between the height of the channel to its width. The effect of variation of the channel height and width has been investigated using the three layer heat sink. Three channel heights have been considered: 500μm, 750μm and 1000μm for fixed channel height (500μm) i.e. the aspect ratios are 1, 1.5 and 2 respectively. Hence, the number of channels in each layer remains the same. The maximum solar cell temperature decreased by 3°C when the channel height was doubled. Also, the fluid pressure drop decreased

dramatically from around 200 Pa for 500µm microchannel height to just 50 Pa for 1000µm microchannel height. This decrease in the pressure drop leads to a reduction in the power required for the fluid pumping as shown in figure 8.

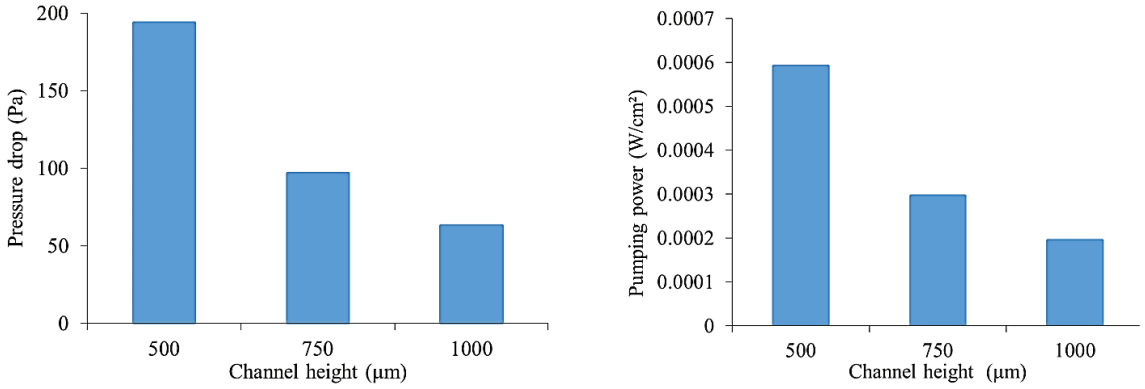

FIGURE 8. Comparison of total heat sink (a) Pressure drop and (b) Pumping power for different microchannel height at fixed mass flow rate (0.002 kg/s).

The effect of the channel width has been investigated by considering three width values 500µm, 750µm and 1000µm for a fixed channel height (500 µm). In this case, the number of channels in each layer increases with the decrease of the channel width. The investigations show that the channel width has no effect on reducing the maximum solar cell temperature (57°C) and the thermal resistance of the heat sink for a fixed fluid mass flow rate (0.002 kg/s). However, the wider channel causes the pressure drop to slightly decrease along the channels as shown in figure 9 (a). An interesting observation is that the fluid pumping power increases as the channel width increases although the pressure drop decreases. This could be understood by the fact that the velocity of the fluid at the channel inlet increases as the channel width increases.

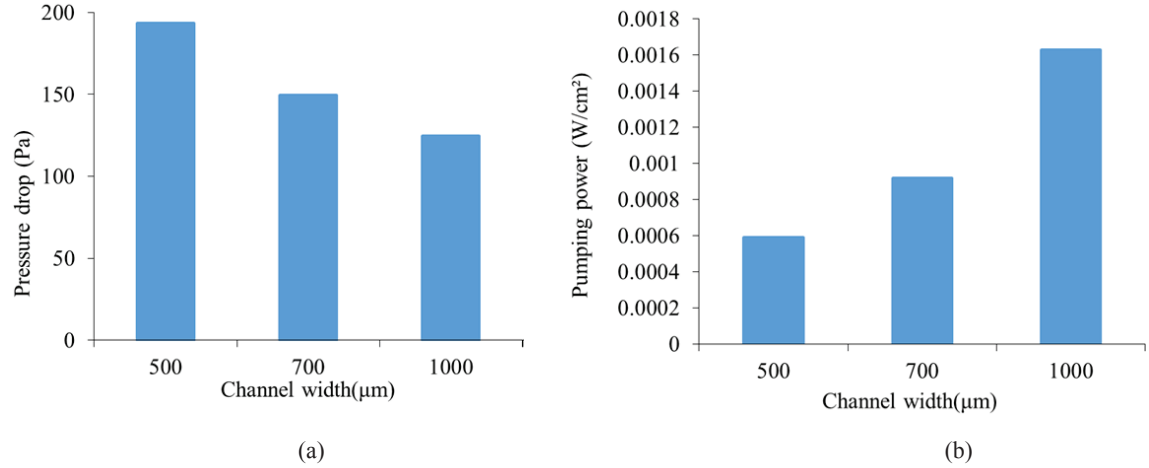

FIGURE 9. Comparison of total heat sink (a) pressure drop and pumping power for different microchannel widths at fixed mass flow rate (0.002 kg/s).

CONCLUSION

In this paper, the concept of multi-layer microchannel heat sinks for CPV applications has been presented, the entire domain (the heat sink and CPV) being considered using a three-dimensional model. The study has

investigated the effect of variation of the number of layers and the channel width and height. The electrical and thermal model has been coupled for an accurate calculation of the generated thermal heat of the solar cell.

The results show a significant improvement of the heat sink performance in terms of the solar cell temperature, the thermal resistance and the fluid pumping power as the number of layers increases for the same total fluid mass flow rate. The three layer microchannel heat sink was considered for the investigation of the channel height and width on the heat sink performance. The results show that the variation of the height of the channel height and the width has no effect on the maximum solar cell temperature. However, the fluid pressure drop along the channel is reduced significantly as the channel height was increased from 500μm to 1000μm i.e. a reduction in fluid pumping power consumption.

The effectiveness of multi-layer microchannel heat sink also depends on other design parameters such as the fluid inlet/outlet manifold and the fluid mass flow rate. In this light, future works will consider further parameters for improvement and optimization of the system efficiency.

ACKNOWLEDGMENT

The PhD scholarship of Idris Al Siyabi is founded by the ministry of higher education at the sultanate of Oman through the national program of postgraduate scholarships.

REFERENCE

1. Micheli L, Micheli L, Fernandez EF, Almonacid F. Enhancing Ultra-High CPV Passive Cooling Using Least-Material Finned Heat Sinks. Cpv-11 2015:3–6.
2. Araki K, Uozumi H, Yamaguchi M. a Simple Passive Cooling Structure and Its Heat Analysis for 500 X 2002:1568–71.
3. Ye Z, Li Q, Zhu Q, Pan W. The cooling technology of solar cells under concentrated system. 2009 IEEE 6th Int Power Electron Motion Control Conf IPEMC '09 2009;3:2193–7. doi:10.1109/IPEMC.2009.5157766.
4. Bahaidarah HMS, Baloch AAB, Gandhidasan P. Uniform cooling of photovoltaic panels: A review. Renew Sustain Energy Rev 2016;57:1520–44. doi:10.1016/j.rser.2015.12.064.
5. Royne A, Dey CJ, Mills DR. Cooling of photovoltaic cells under concentrated illumination: A critical review. Sol Energy Mater Sol Cells 2005;86:451–83. doi:10.1016/j.solmat.2004.09.003.
6. Theristis M, Donovan TSO. An integrated thermal electrical model for single cell photovoltaic receivers under concentration 2014:1–12. doi:10.13140/2.1.3601.3446.
7. Aldossary A, Mahmoud S, Al-Dadah R. Technical feasibility study of passive and active cooling for concentrator PV in harsh environment. Appl Therm Eng 2016;100:490–500. doi:10.1016/j.applthermaleng.2016.02.023.
8. Reddy KS, Lokeswaran S, Agarwal P, Mallick TK. Numerical Investigation of Micro-channel based Active Module Cooling for Solar CPV System. Energy Procedia 2014;54:400–16. doi:10.1016/j.egypro.2014.07.283.
9. Barrau J, Perona A, Dollet A, Rosell J. Outdoor test of a hybrid jet impingement/micro-channel cooling device for densely packed concentrated photovoltaic cells. Sol Energy 2014;107:113–21. doi:10.1016/j.solener.2014.05.040.
10. Wei X, Joshi Y. Stacked Microchannel Heat Sinks for Liquid Cooling of Microelectronic Components. J Electron Packag 2004;126:60. doi:10.1115/1.1647124.
11. Wei X, Joshi Y, Patterson MK. Experimental and Numerical Study of a Stacked Microchannel Heat Sink for Liquid Cooling of Microelectronic Devices. J Heat Transfer 2007;129:1432. doi:10.1115/1.2754781.
12. Toh K., Chen X., Chai J. Numerical computation of fluid flow and heat transfer in microchannels. Int J Heat Mass Transf 2002;45:5133–41. doi:10.1016/S0017-9310(02)00223-5.
13. Ansari D, Kim K-Y. Double-Layer Microchannel Heat Sinks With Transverse-Flow Configurations. J Electron Packag 2016;138:31005. doi:10.1115/1.4033558.
14. COMSOL Multiphysics Reference Guide 2012.
15. Azure Space Solar Power GMBH. Enhanced Fresnel Assembly - EFA Type: 3C42A – with 10x10mm2 CPV TJ Solar Cell Application: Concentrating Photovoltaic (CPV) Modules 2014:0–4.